Broad-band dielectric spectroscopy analysis of relaxational dynamics in Mn-doped $SrTiO_3$ ceramics

A. Tkach, P. M. Vilarinho, and A. L. Kholkin
Department of Ceramics and Glass Engineering, CICECO, University of Aveiro, 3810-193 Aveiro, Portugal

A. Pashkin,* S. Veljko, and J. Petzelt
Department of Dielectrics, Institute of Physics, ASCR, Na Slovance 2, 18221 Prague 8, Czech Republic
(Received 23 October 2005; published 22 March 2006)

Dielectric properties of $Sr_{1-x}Mn_xTiO_3$ ceramics ($x=0-0.15$ and 1) prepared by conventional mixed oxide method were investigated in radio frequency, high frequency, terahertz, and infrared ranges. It is shown that the real and imaginary parts of the dielectric permittivity between 100 Hz and 1 MHz exhibit a relaxation in the temperature range of 30–80 K, shifting to higher temperatures with increasing Mn content. The dielectric relaxation is also observed at higher frequencies (around 100 K for high frequencies and up to room temperature for terahertz frequencies) in $Sr_{0.95}Mn_{0.05}TiO_3$ ceramics. Activation energy $U\sim 52-78$ meV and relaxation time pre-exponent $\tau_0\sim(1-12)\times 10^{-14}$ s are obtained using Arrhenius and Vogel-Fulcher relations. Such dielectric behavior is attributed to Mn off-center relaxation at Sr site of highly polarizable $SrTiO_3$ lattice. Moreover, a reduction of the phonon contribution to the dielectric constant with Mn doping accompanying a stiffening of the soft lattice mode is found in infrared reflectivity spectra and could be related to the interaction of the soft mode with off-centered Mn ions and polar clusters.

DOI: 10.1103/PhysRevB.73.104113 PACS number(s): 61.10.Nz, 68.37.Hk, 68.37.Lp, 77.22.−d

I. INTRODUCTION

Among ferroelectrics of the perovskite type having general formula ABO_3, there exist three materials, $SrTiO_3$ (ST), $KTaO_3$, and $CaTiO_3$,[1] which posses polar soft modes but do not exhibit any ferroelectric phase transition down to 0 K. Due to this fact these crystals are classified as incipient ferroelectrics. Over last decades, there has been a growing interest in studies of dielectric properties of incipient ferroelectrics doped with different impurities.[2] Random lattice disorder produced by chemical substitution in ABO_3 perovskite lattice can lead to the formation of dipolar impurities and defects that influence both static and dynamic lattice properties of these materials. Because of the high polarizability of the ABO_3 host lattice associated with its soft ferroelectric mode, the dipolar entities polarize regions around them forming polar nanodomains or microdomains embedded in nonpolar matrix. When these dipolar entities possess more than one equivalent orientation, they may undergo dielectric relaxation under an applied ac field.[2]

Due to their ionic multivalent state Mn impurity centers in ST lattice can be associated with either Sr or Ti sites. A detailed study of the structure and microstructure of $Sr_{1-x}Mn_xTiO_3$ and $SrTi_{1-y}Mn_yO_3$ has been previously performed by the some of the authors.[3] It was observed that Mn^{2+} ions can occupy Sr sites in a concentration range up to 3%, while the solubility of Mn^{4+} ions at Ti sites is higher than 15%. Moreover, the unit cell parameter of $Sr_{1-x}Mn_xTiO_3$ was found to decrease with increasing Mn concentration 3.7 times slower than that of $SrTi_{1-y}Mn_yO_3$.[3]

A low-temperature dielectric relaxation for $SrTiO_3$:Mn system with Mn concentration up to 0.05 was reported by Lemanov and co-workers, although the lattice site for the dopant occupancy was not clearly stated in that work.[4] The dielectric anomaly was attributed to the reorientation of polarons localized at defects of the $\{Mn_{Ti}^{2+}-O^-\}$ type and its parameters were reported to be insensitive to the dopant concentration,[4] which is in contradiction to the recent publications of some of the present authors.[5,6] A polar dielectric anomaly with corresponding hysteretic response in polarization vs electric field $P(E)$ curves[5] accompanied with high dielectric tunability[3] were observed only for $Sr_{1-x}Mn_xTiO_3$ system. A diffuse low-temperature peak in $\epsilon'(T)$ was induced by Mn doping and shifted to higher temperatures with increasing measurement frequency and amount of Mn.[4] On the other hand, Ti-site Mn doping was found to drive the system away from ferroelectricity.[6]

So, in contrast to $SrTi_{1-y}Mn_yO_3$ system, where Mn doping does not induce any anomaly and just reduces the dielectric permittivity value, a low-temperature dielectric relaxation was observed in $Sr_{1-x}Mn_xTiO_3$ system. It is then important to study and discuss the possible mechanisms underlying the observed relaxation process.

This paper reports on the dielectric relaxation in a broad frequency range (10^2–10^{14} Hz) in disordered incipient ferroelectric $SrTiO_3$ ceramics, where the disorder is primarily produced by Mn impurity at Sr site. The results are discussed, based on the analysis of the dielectric relaxation using Cole-Cole, Arrhenius, and Vogel-Fulcher relations and on the comparison with the dielectric behavior of other ST-based systems.

II. EXPERIMENTAL PROCEDURE

$Sr_{1-x}Mn_xTiO_3$ (SMnT) ceramic samples with $x=0$, 0.0025, 0.005, 0.01, 0.02, 0.03, 0.05, 0.10, 0.15, and 1 were prepared by conventional mixed oxide method, described in

detail elsewhere.[3] All the samples had a density, measured by the Archimedes's method using diethylphthalate as the immersion liquid, of 0.95–0.98 of the theoretical x-ray density, except of $MnTiO_3$ samples that showed a density of about 0.87.

Complex dielectric permittivity in the frequency range of 10^2–10^6 Hz was measured using a precision LCR meter (HP 4284A) under a weak field of ~1 V/mm and a He-closed-cycle cryostat (Displex APD-Cryogenics CH-2) during heating at a rate of 0.75 K/min in the temperature range of 10–300 K. The temperature was controlled by a digital temperature controller (Scientific Instrument model 9650) with silicon diode thermometers. Au was used as the electrode material, being sputtered onto the two faces of the sintered and polished samples.

Cylinder-shaped samples with a diameter of about 1 mm and height of 5–14 mm were used for the dielectric measurements at the high frequency range. The measurements were carried out both as a function of frequency (in the range of 1 MHz–1.8 GHz) and as a function of temperature (in the range of 100–300 K) using a computer controlled high-frequency dielectric spectrometer equipped with an impedance analyzer (HP 4291B), a coaxial sample cell (NOVOCONTROL BDS 2100), and a temperature chamber (Sigma System M18).

Samples for time-domain terahertz (THz) transmission spectroscopy measurements were polished to a thickness of 0.117 mm. A custom-made time-domain THz transmission spectrometer was used to obtain the complex dielectric response of samples, in the range from 3 to 50 cm^{-1} (90–1500 GHz). This spectrometer uses a femtosecond Ti: sapphire laser and (011)-oriented ZnTe crystal as a THz emitter, generating pulses owing to optical rectification effect. The detection of THz waveforms is performed by an electro-optic sampling technique using another ZnTe crystal. A cryostat (Optistat CF) with Mylar windows was used for measurements down to 10 K.

Cylinder-shaped samples with a diameter of 8 mm and thickness of 1 mm were polished for infrared (IR) spectroscopy measurements. Room temperature IR reflectivity spectra were obtained using a Fourier transform spectrometer (Bruker IFS 113v) with pyroelectric deuterated triglycine sulphate detectors in the frequency range of 20–3300 cm^{-1} (0.6–100 THz) with the resolution of 1 cm^{-1}.

III. RESULTS

The temperature dependence of the real ϵ' and imaginary ϵ'' parts of dielectric permittivity of the $Sr_{1-x}Mn_xTiO_3$ ceramic samples at 10 kHz is shown in Fig. 1. Figure 2 presents the variation of the dissipation factor $\tan\delta=\epsilon''/\epsilon'$ of the same samples with temperature in the low-T range of 10–110 K.

Typical quantum paraelectric behavior, i.e., a steep increase of the dielectric constant and leveling-off at high values, as the temperature approaches 0 K, without any frequency dispersion[7] was observed for undoped $SrTiO_3$. In contrast, $MnTiO_3$ behaves as an ordinary dielectric: the frequency independent dielectric constant close to 22 decreases

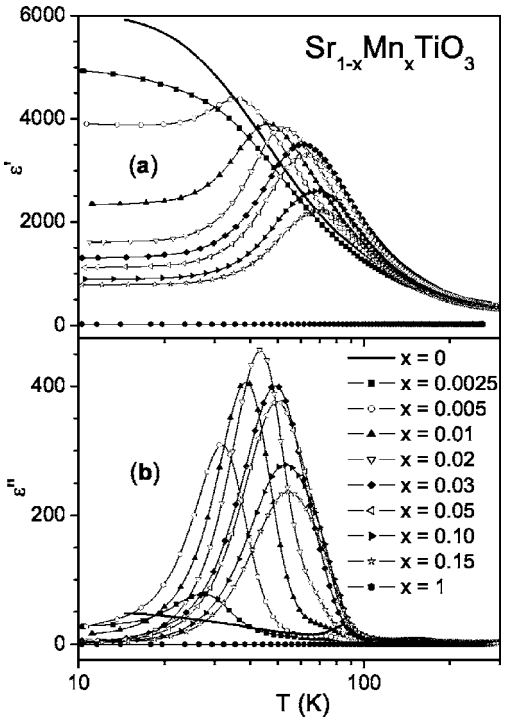

FIG. 1. Temperature dependence of real ϵ' (a) and imaginary ϵ'' (b) parts of the dielectric permittivity of SMnT ceramics at 10 kHz.

with temperature with the slope of $d\epsilon'/dT=1.1\times10^{-3}$ K^{-1}. However, a peak was observed in the temperature dependence of dielectric constant of SMnT samples, starting from $x=0.005$, as shown in Fig. 1(a). Its temperature $T_{\epsilon' m}$ reveals a strong dependence on Mn concentration in the range $x=0.005$–0.03, weakening in the range $x=0.05$–0.15. Such behavior is accompanied by a monotonous decrease of the maximum and low-temperature ϵ' value with x in all the range of Mn concentrations. The inflection point at $x\approx0.03$ in $T_{\epsilon' m}$ vs x dependence coincide with the value of solid solubility limit, obtained by transmission electron microscopy (the solid solubility limit of Mn at Sr sites in the ST lattice determined by XRD was ~10%).[3]

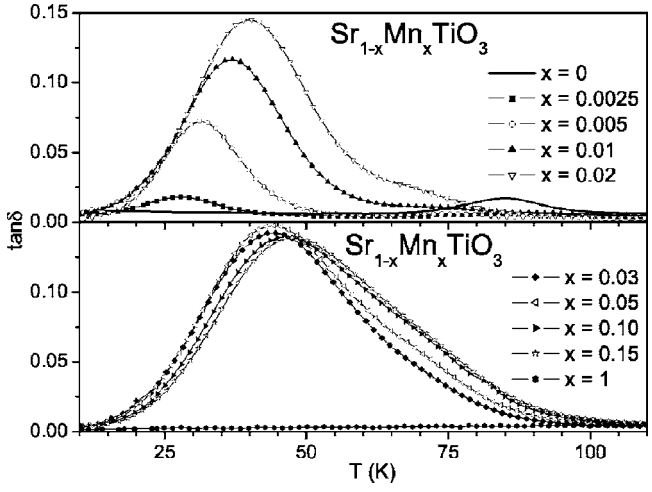

FIG. 2. Temperature dependence of the dissipation factor $\tan\delta$ of SMnT ceramics at 10 kHz.

According to the results depicted in Figs. 1(b) and 2, $MnTiO_3$ exhibits the smallest loss value. The loss of $SrTiO_3$ is slightly higher and characterized by a peak at 70–105 K for the frequency range of 10^2–10^6 Hz that was related to the ferroelastic multidomain state of ST below antiferrodistortive phase transition.[8,9]

Differently, a low-temperature (<70 K) dielectric loss peak was detected for the rest of the SMnT samples, even for the composition with $x=0.0025$, which do not exhibit any dielectric constant anomaly. These peaks are indicative of a strong dielectric relaxation induced by Mn doping. The temperature of the dielectric loss peak is lower than that of the dielectric constant peak, and for both ϵ'' and ϵ', the peak temperature depends on Mn content (strongly in the range of $x=0.0025$–0.03, and weakly in the range of $x=0.05$–0.15). At the same time, the peak value of tan δ increases just in the range of $x=0.0025$–0.02 (from 1.8 to 14.5%), keeping almost the same value ($\sim$14.5%) for the compositions with $x=0.03$–0.15, as shown in Fig. 2.

The effect of Mn doping above $x\approx 0.03$ on the dielectric properties of SMnT ceramics should be considered as a "composite" effect, where the high dielectric permittivity of $Sr_{1-x}Mn_xTiO_3$ (with $x\leqslant 0.03$) is diluted by the low dielectric permittivity of $MnTiO_3$. Therefore permittivity decreases with the Mn concentration as the second phase content increases and the dissipation factor remains almost constant, as previously reported for $Ba_{1-x}Sr_xTiO_3-MgO$.[10,11] However, no effect of the dilution with an ordinary dielectric phase such as $MnTiO_3$ should be expected on the relaxation dynamics of SMnT ceramics.

The effect of the frequency (from 0.1 kHz to 0.2 THz) on the dielectric response of SMnT ceramics is shown in Fig. 3 for the representative composition $Sr_{0.95}Mn_{0.05}TiO_3$. The shift of the dielectric permittivity peak (from $\sim$45 K at 0.1 kHz through $\sim$100 K at 1 GHz to $\sim$170 K at 0.2 THz) is evident, revealing the evolution of the dielectric relaxation. In addition, a decrease of the dielectric constant with frequency, corresponding to the relaxationlike dispersion, was observed in THz range even at room temperature, as shown in detail in the inset of Fig. 4.

Figure 4 presents the spectra in the THz and IR range, obtained at room temperature. IR reflectivity spectra normalized using THz data were fitted using the generalized four-parameter damped multioscillator model of the dielectric function, as shown in Fig. 4(a). Additional three-parameter overdamped oscillator mode was added to take into account the relaxational dispersion below phonon frequencies in $Sr_{0.95}Mn_{0.05}TiO_3$ ceramics.

As is well known,[12] three transverse optic phonon modes TO_1 (soft mode), TO_2 (174 cm^{-1}) and TO_4 (545 cm^{-1}) are observed in the cubic phase of undoped $SrTiO_3$. Mn doping in Sr site causes appreciable changes in far IR spectra. The soft mode monotonously hardens with increasing Mn content: from 90 cm^{-1} for $SrTiO_3$ through 91 cm^{-1} for $Sr_{0.995}Mn_{0.005}TiO_3$ to 102 cm^{-1} for $Sr_{0.95}Mn_{0.05}TiO_3$, as seen from Figs. 4(b) and 4(c). The stiffening of the soft mode is accompanied by the corresponding lowering of the THz permittivity value. Thus, the phonon contribution to the dielectric constant at room temperature decreases monotonously from 302 for $SrTiO_3$ through 298 for $Sr_{0.995}Mn_{0.005}TiO_3$ to

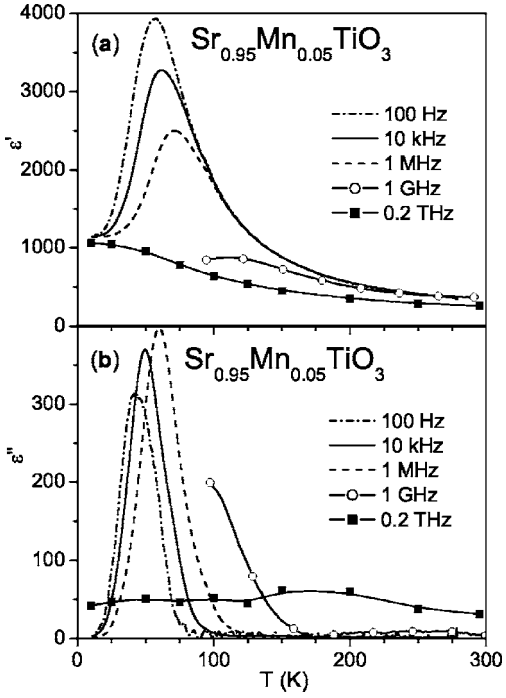

FIG. 3. Temperature dependence of real ϵ' (a) and imaginary ϵ'' (b) parts of the dielectric permittivity of $Sr_{0.95}Mn_{0.05}TiO_3$ ceramics at 100 Hz (dash-dot lines), 10 kHz (solid lines), 1 MHz (dash lines), 1 GHz (open symbols), and 0.2 THz (solid symbols).

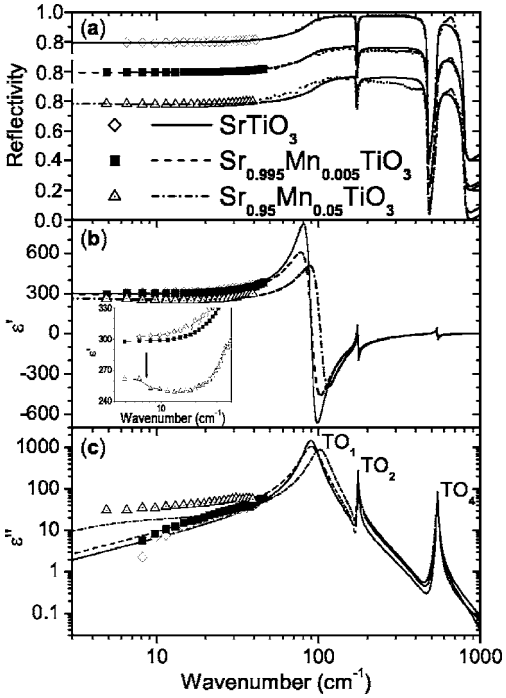

FIG. 4. Room-temperature spectra of IR reflectivity (dot lines) and their fits (a), as well as real and imaginary parts of the dielectric permittivity, ϵ' (b) and ϵ'' (c) calculated from the IR reflectivity fits, for $SrTiO_3$, $Sr_{0.995}Mn_{0.005}TiO_3$, and $Sr_{0.95}Mn_{0.05}TiO_3$, ceramics together with data, obtained by THz transmission spectroscopy. Inset shows THz-range spectra of ϵ' in an expanded scale.

249 for $Sr_{0.95}Mn_{0.05}TiO_3$. The phonon contribution could be suppressed by interaction of the soft mode with the off-centered ions and polar clusters, in analogy with $Sr_{1-1.5x}Bi_xTiO_3$ and $Ka_{1-x}Li_xTaO_3$ systems.[13]

IV. DISCUSSION

In order to clarify the nature of the dielectric relaxation induced by Mn ions in ST lattice a detailed analysis of the present experimental dielectric data of SMnT system in terms of different dielectric relaxation models and comparison with relaxation mechanisms reported for other ST-based systems will be performed in this section.

Frequency dependence of the dielectric constant $\epsilon'(f)$ and loss $\epsilon''(f)$ of SMnT samples with $x=0.02$ and 0.05 at different temperatures are shown in Figs. 5(a), 5(c), and 5(d) in a semilogarithmic scale. The relaxation-type dispersion is evident. The frequency of the loss peak increases with temperature, indicating that the microscopic process that leads to the dielectric anomaly, is a thermally activated polar motion.

It is known that many dielectric relaxation processes are broader than simple Debye model and can be described by the Cole-Cole equation

$$\epsilon^*(\omega) = \epsilon_\infty + [\epsilon_{dc} - \epsilon_\infty]/[1 + (i\omega\tau)^{1-\alpha}], \quad 0 \leqslant \alpha \leqslant 1 \quad (1)$$

with a simple Arrhenius expression for the relaxation time

$$\tau = \tau_0 \exp(U/k_B T). \quad (2)$$

Here, $\epsilon^* = \epsilon' - i\epsilon''$, ϵ_{dc} stands for the permittivity at zero frequency, ϵ_∞ stands for the permittivity at infinite frequency, $\omega = 2\pi f$ stands for the angular frequency, α stands for the angle of the semicircular arc (an empirical parameter describing diffuseness of the spectrum), τ_0 stands for the pre-exponential term or inverse attempt frequency, U stands for the activation energy, k_B stands for the Boltzmann constant, and T stands for the temperature. The α value represents the deviation from the ideal Debye model.

TABLE I. Relaxation dynamics parameters of SMnT compositions.

		Arrhenius law		Vogel-Fulcher relation		
x	α	U, meV	τ_0, s	U, meV	τ_0, s	T_f, K
0.0025	~0.68	34	8.8×10^{-12}			
0.005	~0.68	52	6.6×10^{-14}			
0.01	~0.73	69	1.3×10^{-14}			
0.02	~0.70	73	3.8×10^{-14}			
0.03	~0.76	85	1.6×10^{-14}	78	4.0×10^{-14}	2.2
0.05	~0.80	91	4.4×10^{-15}	71	5.0×10^{-14}	5.8
0.10	~0.81	99	1.1×10^{-15}	73	7.8×10^{-14}	5.0
0.15	~0.81	107	2.1×10^{-16}	64	11.6×10^{-14}	10.1

The Cole-Cole plots (ϵ'' versus ϵ') are presented for $x=0.02$ ceramics at different temperatures in Fig. 5(b), corresponding to the data of Fig. 5(a). The values of the diffuseness parameter α were obtained by fitting to Eq. (1) and are shown in Table I. α was found to be about 0.70 ± 0.03, yet increasing with increasing x. Such high α values correspond to a high diffuseness of the dielectric spectra $\epsilon(f)$, or in other

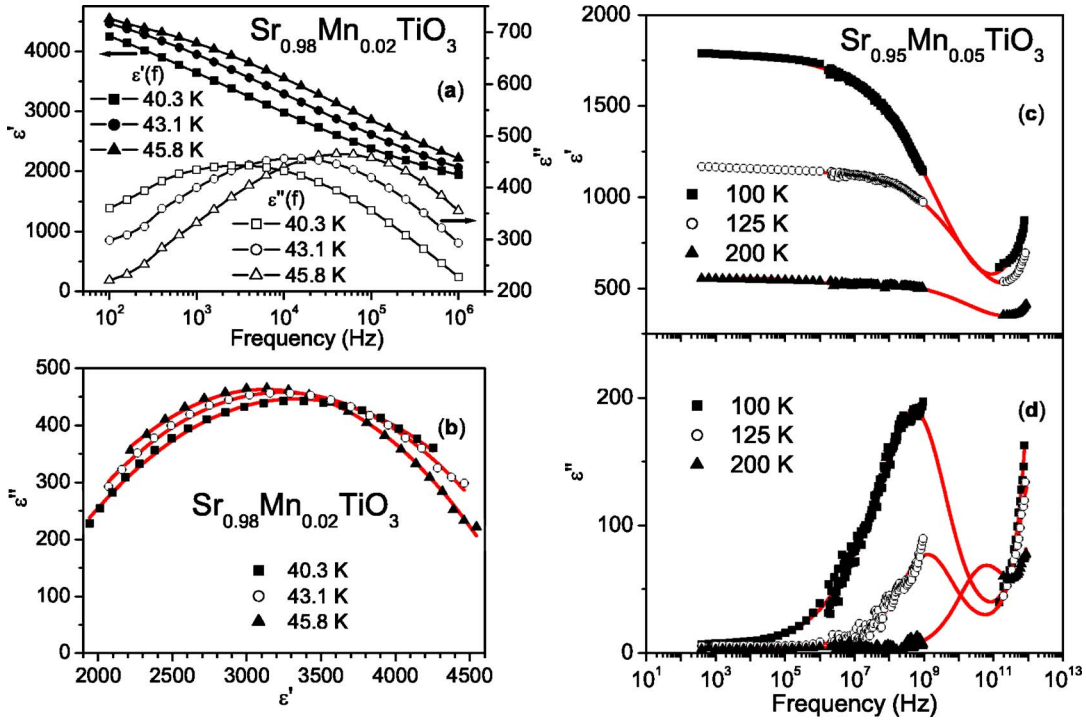

FIG. 5. (Color online) Low-frequency spectra of real ϵ' and imaginary ϵ'' parts of the dielectric permittivity (a) and corresponding Cole-Cole plots ϵ' vs ϵ'' together with their fits (b) of $Sr_{0.98}Mn_{0.02}TiO_3$ and wide-frequency spectra of ϵ' (c) and ϵ'' (d) of $Sr_{0.95}Mn_{0.05}TiO_3$ ceramics at different temperatures. The lines in (c) and (d) are to guide the eyes.

words, to a wide-range distribution of relaxation times, still increasing in the high x range.

Relaxation time pre-exponents and other parameters of the relaxation dynamics were deduced from the frequency and temperature values of the ϵ'' peak. In a dielectric material, if the dielectric relaxation process is governed by a thermally activated motion, the temperature dependence of the relaxation time follows the Arrhenius law [Eq. (2)]. For SMnT samples with $x=0.0025$–0.05, the Arrhenius plots $\ln(\tau)=\ln(\omega^{-1})$ versus $1000/T_{\epsilon''m}$ are presented in Fig. 6. The data points can be fitted by straight lines, whose position and slope vary monotonously with Mn content for $x=0.0025$–0.02, being almost coincident for $x=0.03$–0.15.

The activation energy U and the pre-exponential term τ_0 values, obtained for all the SMnT samples by fitting to the Arrhenius law in the frequency window of 10^2–10^6 Hz, are presented in Table I. In the case of $x=0.005$–0.02, Arrhenius law parameters $U=52$–73 meV and $\tau_0 \sim (1$–$7)\times 10^{-14}$ s were obtained. Such parameters are rather different from the activation energy $U \approx 30$ meV and the relaxation time $\tau_0 \approx 5\times 10^{-11}$ s reported by Lemanov and co-workers for $SrTiO_3$:Mn system and attributed to the reorientation of polarons localized at defects of the $\{Mn_{Ti}^{2+}-O^{-}\}$ type.[4] Much closer values for the same parameters were obtained in $Sr_{1-1.5x}Bi_xTiO_3$ system for small x and related to a relaxation of noninteracting off-center dopant dipoles.[4] In the same way, the contribution of individual off-center Mn^{2+} ions can dominate in the $Sr_{1-x}Mn_xTiO_3$ system. The somewhat smaller τ_0 and U parameters for the $Sr_{0.9975}Mn_{0.0025}TiO_3$ composition can be explained both by the difficulty of precise quantitative description of the loss peak due to its weakness and by the possible overlapping between the thermally activated and quantum tunnelling regimes of the off-center ions motion at low temperatures,[8] included in the overall picture of relaxation dynamics. Thus, the results showed that Mn^{2+} substitutes at the Sr^{2+} site, but spontaneously displaces off-center forming a strong dipole that hops among equivalent positions with an activation energy of 62 ± 10 meV.

In the case of $x=0.03$–0.15, the activation energy of $U=85$–107 meV and pre-exponential term $\tau_0=(0.2$–$16)\times 10^{-15}$ s were obtained by fitting to Arrhenius law. However, τ_0 values $\sim 10^{-15}$ s are close to the electronic reciprocal collision time and seem to be physically unreasonable. Fitting to Arrhenius law also yielded too small τ_0 for $KTa_{1-y}Nb_yO_3$ at a Nb concentration $y=0.009$.[2] Due to this, a cooperative freezing mechanism affecting the Nb motion was suggested and the average relaxation time of reorientation of Nb-induced clusters was obtained by the Vogel-Fulcher relation

$$\tau = \tau_0 \exp[U/k_B(T_m - T_f)]. \quad (3)$$

Compared to Arrhenius law, this relation includes one additional fitting parameter T_f, interpreted as a static freezing temperature, at which motion of all dipole moments slows down, and is often used to describe the behavior of relaxor polar clusters or strongly correlated dipoles. In SMnT system, it is reasonable to admit that the dipoles, created by the off-center Mn dopant, might correlate through the highly polarizable host lattice for Mn contents higher than a certain value and therefore the polar clusters might be formed. Fitting the data to Vogel-Fulcher relation yields the relaxation time τ_0 and the activation energy U values equal to $(7.8\pm 3.8)\times 10^{-14}$ s and 71 ± 7 meV, respectively, which seems to be more realistic, compared to the results obtained from the fitting to Arrhenius law. The freezing temperature T_f slightly increases with Mn content, reaching 10 K at $x=0.15$. The obtained values are also listed in Table I. It is worthwhile to mention here that fitting the data of $Sr_{1-x}Mn_xTiO_3$ ceramics with $x<0.03$ to Vogel-Fulcher relation had no stable solution. Based on this observation, although for $x=0.03$ the solid solubility of Mn in Sr sites of ST lattice was reached, it is proposed that at $x=0.03$ also a crossover from hopping of individual off-center Mn^{2+} ions to a polar clusters reversal dominant mechanism of relaxational dynamics occurs. This idea is supported by a sudden increase of the α value at $x=0.03$.

In addition, parameters of the dielectric relaxation dynamics of $Sr_{0.95}Mn_{0.05}TiO_3$ ceramics in high-frequency and THz ranges were also deduced from the frequency and temperature values of the ϵ'' peak at these frequencies. As shown in Fig. 6, fitting to Vogel-Fulcher relation with parameters obtained in the low-frequency range can be extrapolated to the data in the high-frequency range in good accordance.

Several mechanisms have been proposed for the dielectric relaxations observed in other ST-based systems.[14–20] Some of them are listed in Table II together with corresponding values of U and τ_0 parameters, obtained by fitting to the Arrhenius law.

The interfacial polarization of the Maxwell-Wagner type, reported to be the mechanism of relaxation in $SrTiO_3$ and $BaTiO_3$,[15] could also be detected in $Sr_{1-x}Mn_xTiO_3$ system, as in any ceramics with grains and grain boundaries, that possess different electric properties. However, the Maxwell-Wagner type relaxation is usually ~ 10 orders of magnitude slower and its activation energy is ~ 10 times higher[15] than those here obtained. Much higher activation energy was also reported for low-frequency dielectric relaxations attributed to oxygen vacancies[19,20] and to ionic polarization of Skanavi model in $Sr_{1-1.5x}Bi_xTiO_3$, $SrTiO_3-SrMg_{1/3}Nb_{2/3}O_3$, $SrTiO_3$

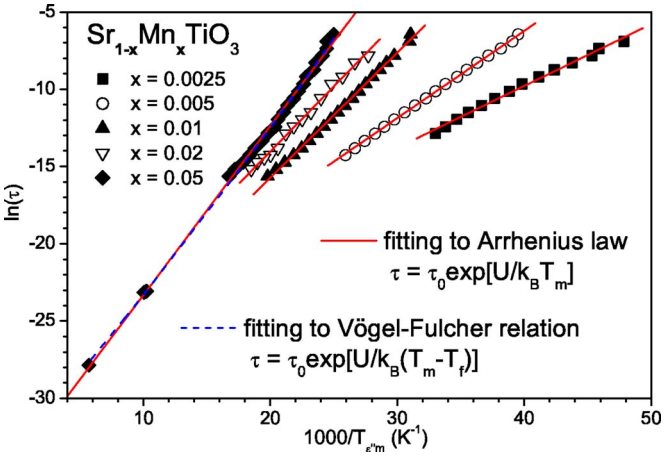

FIG. 6. (Color online) Arrhenius plots $\ln(\tau)$ vs $1000/T_{\epsilon''m}$ ($T_{\epsilon''m}$ is the temperature at which the maximum of ϵ'' occurs at the angular frequency $\omega=2\pi f$; $\tau=\omega^{-1}$) for SMnT ceramics with fits to Arrhenius law and Vogel-Fulcher relation.

TABLE II. Relaxation mechanisms observed in ST-based systems and their Arrhenius-law parameters.

System	U, meV	τ_0, s	Proposed mechanism	Ref.
$SrTiO_3$, $BaTiO_3$	700	$(2-6)\times10^{-2}$	Interfacial polarization of the Maxwell-Wagner type	15
Ba:$SrTiO_3$	40–45	5×10^{-12}–5×10^{-10}	Electronic process of unknown nature	16
	100–120	$10^{-11}-10^{-10}$	Off-center ion hopping between symmetry equivalent position	16
Ca:$SrTiO_3$	11–15	$(1.4-2.3)\times10^{-10}$	Nanoregions around dilute off-center dopant dipoles	17 and 18
Bi:$SrTiO_3$	32–34 60–64	$(0.4-2)\times10^{-13}$ $(0.4-1)\times10^{-13}$	Noninteracting polar clusters formed by off-center dopant ions with and without Sr vacancy nearby	14
	300–900	$(0.5-7)\times10^{-12}$	Oxygen-vacancy-related low-frequency dielectric relaxation	19
$SrTiO_3$-$SrMg_{1/3}Nb_{2/3}O_3$, $SrTiO_3$-$SrSc_{1/2}Ta_{1/2}O_3$	210–300	$(0.2-5)\times10^{-11}$	Oxygen-vacancy-related low-frequency dielectric relaxation	20
	10–20	$(0.2-15)\times10^{-9}$	Polaronic relaxation	20
ST doped with rare-earth ions	212–496	7×10^{-14}–9×10^{-10}	Ionic polarization of Skanavi model	21

$-SrSc_{1/2}Ta_{1/2}O_3$, and ST doped with rare-earth ions, respectively.[21] The latter model postulates the appearance of more than one off-center equilibrium position for Ti ion due to the distortions introduced in the perovskite lattice by rare-earth ions with 3+ charge state and associated Sr-site vacancies. Thermally activated motion between these equivalent minima leads to the observed relaxation. According to the Skanavi model, activation energy is expected to increase with increasing dopant concentration, which in turn promotes an increase of the lattice distortions. However, these aforementioned models might not be applicable to SMnT system, since their relaxational dynamics follows only to the Arrhenius law, whereas the relaxational dynamics in SMnT seems to undergo a crossover from Arrhenius law to Vogel-Fulcher relation.

The relaxation dynamics of SMnT system is very similar to that of $Sr_{1-1.5x}Bi_xTiO_3$, in which the Vogel-Fulcher relation can be applicable starting from $x=0.04$.[14] Therefore, the relaxation was related to dynamic polar nanoclusters, created by the off-centered dopant ions interacting via crystal lattice, i.e., correlated motion of the off-centered dopant ions.[13] Below that concentration, the dispersion in Bi-doped ST, is better described by Arrhenius law with parameters very close to those of SMnT system.[14] Moreover, the origin of this relaxation in $Sr_{1-1.5x}Bi_xTiO_3$, and consequently in $Sr_{1-x}Mn_xTiO_3$, is similar to that of the $K_{1-x}Li_xTaO_3$, i.e., off-center dopant relaxation at A site of highly polarizable perovskite lattice.[13]

In addition, a low-temperature relaxation with $U=75$ meV and $\tau_0\sim10^{-14}$ s, independently on the substitution impurity and its concentration, was observed in many perovskite crystals and ceramics and was proposed to be due to a polaronic mechanism.[22] However, the undoped and Ca-doped ST (for which the dielectric loss peaks appeared around 10–13 K) could not be described by the Arrhenius law with similar parameters. Regarding SMnT system presented in this work, several misfits between the observed behavior and polaronic model are evident. Arrhenius law is well applicable for SMnT with Mn content $x<0.03$, but with activation energy increasing with x, which is in contradiction to almost invariant values of U and τ_0 obtained for polaronic mechanism.[22] On the other hand, U and τ_0 close to 75 meV and $\tau_0\sim10^{-14}$ s, respectively, were obtained for SMnT with $x\geqslant0.03$, but using fitting with Vogel-Fulcher relation.

V. CONCLUSIONS

The relaxor-type dielectric behavior observed for SMnT ceramics was attributed to the off-center hopping of Mn^{2+} ions at Sr sites of highly polarizable $SrTiO_3$ lattice. This conclusion was supported by the dielectric spectroscopy and dielectric relaxation analysis conducted in this work. It was observed that the contribution of individual off-center Mn^{2+} ions dominates the dielectric spectra at lower concentrations $x<0.03$ and can be described by the Arrhenius law with the activation energy $U\sim52$–73 meV and the relaxation time $\tau_0\sim(1-7)\times10^{-14}$ s, whereas the contribution of the polar clusters, induced by the off-centered ions interacting via crystal lattice, prevail at higher Mn concentrations in the dielectric spectra and can be described by Vogel-Fulcher relation with the $U\sim64$–78 meV, $\tau_0\sim(4-12)\times10^{-14}$ s, and

freezing temperature $T_f \sim 2$–10 K. Although for the SMnT ceramics $x=0.03$ corresponds to the solid solubility limit it correlates well with the scheme of the dielectric behavior of moderately doped incipient ferroelectrics, constructed from the analysis of dielectric spectra of $K_{1-x}Li_xTaO_3$ and $Sr_{1-1.5x}Bi_xTiO_3$ by Bovtun *et al.*[13] In addition, dielectric relaxation is observed also at high frequencies and can be detected in SMnT ceramics even in the THz range. Moreover, time-domain THz and IR spectra reveal that the soft mode shifts to higher frequencies and the soft mode phonon contribution to the dielectric response becomes smaller with increasing concentration of the Mn^{2+} ions, being suppressed by the interaction with off-centered ions and polar clusters in full agreement with the model proposed by Bovtun *et al.*[13]

ACKNOWLEDGMENTS

Alexander Tkach acknowledges FCT (Portuguese Foundation for Science and Technology) for financial support. The work was also supported by the Czech Grant Agency GACR (Project No. 202/04/0993) and the COST 525 program.

*Present address: Physikalishes Institut, Universitat Stuttgart, D-70550 Stuttgart, Germany.

[1] V. V. Lemanov, A. V. Sotnikov, E. P. Smirnova, M. Weihnacht, and R. Kunze, Solid State Commun. **110**, 611 (1999).
[2] B. E. Vugmeister and M. D. Glinchuk, Rev. Mod. Phys. **62**, 993 (1990).
[3] A. Tkach, P. M. Vilarinho, and A. L. Kholkin, Acta Mater. **53**, 5061 (2005).
[4] V. V. Lemanov, E. P. Smirnova, A. V. Sotnikov, and M. Weihnacht, Fiz. Tverd. Tela (S.-Petersburg) **46**, 1442 (2004) [Phys. Solid State **46**, 1442 (2004)].
[5] A. Tkach, P. M. Vilarinho, and A. L. Kholkin, Appl. Phys. Lett. **86**, 172902 (2005).
[6] A. Tkach, P. M. Vilarinho, and A. L. Kholkin, Ferroelectrics **304**, 917 (2004).
[7] K. A. Müller and H. Burkard, Phys. Rev. B **19**, 3593 (1979).
[8] R. Viana, P. Lunkenheimer, J. Hemberger, R. Bohmer, and A. Loidl, Phys. Rev. B **50**, 601(R) (1994).
[9] C. Ang, R. Guo, A. S. Bhalla, and L. E. Cross, J. Appl. Phys. **87**, 3937 (2000).
[10] B. Su and T. W. Button, J. Appl. Phys. **95**, 1382 (2004).
[11] L. C. Sengupta and S. Sengupta, Mater. Res. Innovations **2**, 278 (1999).
[12] J. Petzelt, T. Ostapchuk, I. Gregora, I. Rychetský, S. Hoffmann-Eifert, A. V. Pronin, Y. Yuzyuk, B. P. Gorshunov, S. Kamba, V. Bovtun, J. Pokorný, M. Savinov, V. Porokhonskyy, D. Rafaja, P. Vaněk, A. Almeida, M. R. Chaves, A. A. Volkov, M. Dressel, and R. Waser, Phys. Rev. B **64**, 184111 (2001).
[13] V. Bovtun, V. Porokhonskyy, M. Savinov, A. Pashkin, V. Zelezny, and J. Petzelt, J. Eur. Ceram. Soc. **24**, 1545 (2004).
[14] C. Ang and Z. Yu, J. Appl. Phys. **91**, 1487 (2002).
[15] H. Neumann and G. Arlt, Ferroelectrics **69**, 179 (1986).
[16] A. V. Sotnikov, V. V. Lemanov, E. P. Smirnova, M. Weihnacht, and R. Kunze, Ferroelectrics **223**, 113 (1999).
[17] U. Bianchi, J. Dec, W. Kleemann, and J. G. Bednorz, Phys. Rev. B **51**, 8737 (1995).
[18] W. Kleemann, A. Albertini, R. V. Chamberlin, and J. G. Bednorz, Europhys. Lett. **37**, 145 (1997).
[19] C. Ang, Z. Yu, and L. E. Cross, Phys. Rev. B **62**, 228 (2000).
[20] V. V. Lemanov, E. P. Smirnova, A. V. Sotnikov, and M. Weihnacht, Appl. Phys. Lett. **77**, 4205 (2000).
[21] D. W. Johnson, L. E. Cross, and F. A. Hummel, J. Appl. Phys. **31**, 2828 (1970).
[22] O. Bidault, M. Maglione, M. Actis, M. Kchikech, and B. Salce, Phys. Rev. B **52**, 4191 (1995).